

Spatially Inhomogeneous Population Dynamics: Beyond Mean Field Approximation

Igor Omelyan¹ and Yuri Kozitsky²

¹*Institute for Condensed Matter Physics, National Academy of Sciences of Ukraine, 1 Svientsitskii Street, UA-79011 Lviv, Ukraine and*

²*Instytut Matematyki, Uniwersytet Marii Curie-Skłodowskiej, 20-031 Lublin, Poland*

(Dated: January 26, 2019)

We propose a novel method for numerical modeling of inhomogeneous spatial moment dynamics of population systems within a continuous-space model with nonlocal dispersal and competition. It is based on analytical decompositions of the time evolution operator for the coupled set of kinetic equations. This has allowed us to perform first population dynamics simulations of such a type and to calculate the one- and two-order distribution functions in the spatially inhomogeneous case for the first time using the three-order Kirkwood superposition ansatz. We show that the spatial structure of population density and other properties can differ qualitatively from those obtained within the simple mean field approximation which is usually applied to population dynamics by ignoring the two-order correlations. The strong clustering followed by the deep disaggregation in the wavefront of spatial propagation for systems with short-range dispersal or long-range competition are identified. In the opposite regime, the asymmetric long-tail behavior of the inhomogeneous pair correlation function is predicted.

PACS numbers: 87.10.Ed, 87.17.Aa, 87.18.Ed, 87.23.Cc

Population dynamics (PD) is widely used in biology, ecology, medicine, life sciences to study various processes and phenomena [1–3]. Many models have been proposed over the long history of PD. They include continuum, lattice, individual, spatial, and other approaches [1, 2]. While the continuum and lattice schemes are too simplified or specific, the individual-based models (IBMs) in continuous space provide a more detailed description. However, they can be exploited only for systems with a small number of interacting individuals. When the population size increases, the IBMs quickly become inefficient because of the huge computational costs.

Over the last two decades there has been an increasing interest in the development of spatial moment dynamics (SMD) to overcome the drawbacks of the existing PD models [4–12]. In SMD, the properties of a population are represented by time-dependent spatial moments of the distribution. The first two of them are the local population density and pair correlations between entities. The SMD description can be considered as an extension of the traditional mean-field (MF) assumption that is invoked for most models. MF implies that any impact of the spatial structure on the dynamics of the system is completely neglected. Instead, in the SMD approach this impact is easily accounted by the two-, three-, and higher-order correlations.

The SMD models have been applied to ecological dynamics, spatial epidemics, surface chemistry reactions, predator-prey metapopulations ([2, 9] and references herein). They are particularly useful to describe patchiness and clustering [13, 14] in the spatial distribution of different organisms, such as trees in a beech forest [15] or breast cancer cells during an in vitro growth-to-confluence assay [16]. In other words, the SMD approach is able to predict subtle effects which are inaccessible for other PM models. It can also be employed to improve or revisit some MF data, e.g., on the formation of patterns in evolution of bacterial colonies [17].

The SMD description is exact provided the infinite number of spatial moments are involved in the hierarchy of the kinetic equations. For the practical reason, this hierarchy needs to be closed. Usually the closure is performed for three-order

correlations, so that numerical solutions are found for the first two equations. This is quite enough for most applications and much more precise than the MF description. Several closures of powers one, two, and three have been introduced for SMD models [5, 6, 11, 12]. It has been noticed that their accuracy increases with increasing the power number.

Despite the above achievements, all the previous SMD simulations have been restricted to the spatially homogeneous case exclusively. This can be explained by the incapability of the standard numerical methods to solve the second equation for the two-order distribution function at the spatially inhomogeneous conditions. To simplify calculations, it was assumed that the population density does not change in space. On the other hand, even the MF models can deal with the spatial inhomogeneity (while neglecting the pair correlations). This is an obvious limitation of the homogeneous SMD description, since many important properties become impossible to investigate. For instance, the account of spatial inhomogeneity is necessary to study the spread and wavefront dynamics.

In this Letter we present a novel approach to time integration of the kinetic equations for inhomogeneous SMD (ISMD) models. As a result, the first ISMD simulations have been implemented and new effects have been identified.

The two coupled kinetic integro-differential equations of an ISMD model [7, 11, 12] are of the form

$$\frac{dn_t(x)}{dt} = \int dy [a(x, y)n_t(y) - b(x, y)u_t(x, y)] - mn_t(x), \quad (1)$$

$$\begin{aligned} \frac{du_t(x, y)}{dt} &= a(x, y)(n_t(x) + n_t(y)) - 2b(x, y)u_t(x, y) \\ &+ \int dz [a(x, z)u_t(y, z) + a(y, z)u_t(x, z) \\ &- (b(x, z) + b(y, z))w_t(x, y, z)] - 2mu_t(x, y), \end{aligned} \quad (2)$$

where $n_t(x)$, $u_t(x, y)$, and $w_t(x, y, z)$ denote the one-, two- and three-order distribution functions, respectively. The latter change in time t and depend on the corresponding num-

ber of spatial coordinates x, y, z of a certain dimensionality d . The dispersal $a(x, y)$ and competition $b(x, y)$ kernels are commonly given by the Gaussians $c_{\pm}/(2\pi\sigma_{\pm}^2)^{d/2} \exp[-(x-y)^2/(2\sigma_{\pm}^2)]$ with c_{\pm} and σ_{\pm} being the intensities and ranges of the interactions, respectively. These kernels describe the nonlocal processes of birth (+) and death (−) of entities in a population, while m is the intrinsic mortality. The interactions can also be modelled by the square function $c_{\pm}/(\eta_d\sigma_{\pm}^d)$ for $|x-y| \leq \sigma_{\pm}$, becoming zero at $|x-y| > \sigma_{\pm}$, where $\eta_d = 2, \pi, \text{ or } 4\pi/3$ for $d = 1, 2, \text{ or } 3$ to provide the normalization $\int \{a, b\}(x, y)dy = c_{\pm}$.

Although more complex ISMD schemes can be considered too [11, 12], Eqs. (1) and (2) are quite general. In simplified limits they transform to the equations of previous PD models. For example, neglecting any pair correlations by putting $u_t(x, y) \approx n_t(x)n_t(y)$, we come in Eq. (1) to the well-known spatial MF model [18, 19]. Additionally letting $\sigma_+ \rightarrow +0$ we have $\int a(x, y)n_t(y)dy \rightarrow c_+n_t(x) + D\partial^2 n_t(x)/\partial x^2$, leading to the diffusion MF model [17], where $D = c_+\sigma_+^2/2$ is the diffusion coefficient. Finally, for $b(x, y) = c_-\delta(x-y)$ we reproduce from Eq. (1) the classical Fisher-Kolmogorov [20] reaction-diffusion equation $dn_t(x)/dt = D\partial^2 n_t(x)/\partial x^2 + (c_+ - m)n_t(x) - c_-\delta(x-y)n_t^2(x)$.

Despite the importance of the ISMD equations (1) and (2), there were no successful attempts reported on finding their solutions. The reason is that they are rather complicated to be handled by existing numerical methods. Because of this, the crude assumption that $n_t(x)$ does not change on x was made [5, 6, 11, 12]. Then the two-order function $u_t(x, y)$ becomes dependent only on $|x-y|$, simplifying significantly the computations and enabling to obtain the spatially homogeneous results. As was mentioned, the homogeneous approach is very restrictive in comparison with ISMD. The limitations of the former were pointed out also in Ref. [21], where estimations of the inhomogeneous pair correlations were composed. Our method is grounded on the theoretically rigorous framework.

The main concepts of our ISMD approach consist in the following. Firstly, we write down the discrete duplicate of Eqs. (1) and (2) as $dn_i/dt = h \sum_j (a_{ij}n_j - b_{ij}n_{ij}) - mn_i$ and $du_{ij}/dt = a_{ij}(n_i + n_j) - 2(m + b_{ij})u_{ij} + h \sum_k (a_{ik}u_{jk} + a_{jk}u_{ik} - (b_{ik} + b_{jk})u_{ijk})$. Here the sums represent the spatial integrals, while $n_i = n_t(x_i)$, $u_{ij} = u_t(x_i, x_j)$, and $w_{ijk} = w_t(x_i, x_j, x_k)$ are values of the distribution functions in points $x_{i,j,k}$ uniformly distributed over the interval $[-L/2, L/2]$ with spacing $h = L/N$ for all dimensions, $\{a, b\}_{ij} = \{a, b\}(x_i, x_j)$, and $i, j, k = 1, 2, \dots, N$. The number N of points must be large enough to minimize the discretization uncertainties by the smallness of h . The interval L should be sufficiently long to neglect the finite-size effects. Then nonzero values of the distribution functions do not reach the boundaries of the L -region during the finite simulation time T . This corresponds to the Dirichlet boundary conditions $\{n, u\} = 0$ at $x, y \rightarrow \pm\infty$. Secondly, we apply the power-3 [5, 6] closure $w_{ijk} = u_{ij}u_{ik}u_{jk}/(n_i n_j n_k)$ for the third-order correlations. It is well-known [22] in theoretical physics as

the Kirkwood superposition approximation (KSA). Thirdly, we introduce the space $\Gamma = \{n_i, u_{ij}\}$ of dynamical variables. Then the ISMD equations (1) and (2) can be cast in the Liouville form $d\Gamma/dt = \Psi\Gamma$, where $\Psi = \sum_{i=1}^N \Psi_i + \sum_{i \leq j}^N \Psi_{ij}$ is the differential operator with the components

$$\begin{aligned} \Psi_i &= (\alpha_i + \beta_i n_i) \partial / \partial n_i, & \Psi_{ij}^I &= (\alpha_{ij} + \beta_{ij} u_{ij}) \partial / \partial u_{ij}, \\ \Psi_{ij}^{II} &= \gamma_{ij} u_{ij}^2 \partial / \partial u_{ij}, & \Psi_{ii}^{II} &= \zeta_{ii} u_{ii}^3 \partial / \partial u_{ii}, \end{aligned} \quad (3)$$

$\Psi_{ij} = \Psi_{ij}^I + \Psi_{ij}^{II}$, and $\Psi_{ii} = \Psi_{ii}^I + \Psi_{ii}^{II}$. The decomposition coefficients in Eq. (3) are

$$\begin{aligned} \alpha_i &= h \sum_{j \neq i} (a_{ij}n_j - b_{ij}u_{ij}) - hb_0 u_{ii}, & \beta_i &= ha_0 - m, \\ \alpha_{ij} &= a_{ij}(n_i + n_j) + h \left(\sum_{k \neq i} a_{ik}u_{jk} + \sum_{k \neq j} a_{jk}u_{ik} \right), \\ \beta_{ij} &= -2(m + b_{ij}) + h \left(2a_0 - \sum_{k \neq i, j} (b_{ik} + b_{jk}) \frac{u_{ik}u_{jk}}{n_i n_j n_k} \right), \\ \gamma_{ij} &= -\frac{b_0 + b_{ij}}{n_i n_j} \left(\frac{u_{ii}}{n_i} + \frac{u_{jj}}{n_j} \right), & \zeta_{ii} &= -\frac{2hb_0}{n_i^3}, \end{aligned} \quad (4)$$

where a_0 and b_0 designate the kernel values $\{a, b\}_{ii}$.

In view of the above, the solution to the ISMD equations is $\Gamma(t) = [e^{\Psi\Delta t}]^K \Gamma(0)$, where Δt and $K = t/\Delta t$ denote the time increment and total number of steps, respectively. Since the time evolution operator $e^{\Psi\Delta t}$ cannot be handled exactly, we derive the decomposition propagation (DP):

$$e^{\Psi\Delta t} = \prod_{i,j=1}^N e^{\Psi_{ij}\frac{\Delta t}{2}} \prod_{i=N}^1 \prod_{i=1}^N e^{\Psi_i\frac{\Delta t}{2}} \prod_{i,j=N}^1 e^{\Psi_{ij}\frac{\Delta t}{2}} + \mathcal{O}(\Delta t^3). \quad (5)$$

Here the factorization is performed symmetrically with respect to i and i, j , while $i \leq j$ because of $u_t(y, x) = u_t(x, y)$, i.e., $u_{ji} = u_{ij}$. Due to the special decomposition [Eq. (3)] of Ψ , now each of the single exponentials appearing in Eq. (5) can be evaluated analytically. Indeed, the coefficients α_i and β_i for every i do not depend on n_i , as this follows from Eq. (4). Then according to Eq. (3), the operator $e^{\Psi_i\Delta t/2}$ acting on the local density n_i results in the analytical solution

$$e^{\Psi_i\frac{\Delta t}{2}} n_i = n_i e^{\beta_i \Delta t/2} + \alpha_i (e^{\beta_i \Delta t/2} - 1) / \beta_i. \quad (6)$$

Also, the coefficients $\{\alpha, \beta, \gamma\}_{ij}$ or ζ_{ii} for each set ij do not depend on u_{ij} or u_{ii} . Thus, $e^{\Psi_{ij}\frac{\Delta t}{2}} = e^{\Psi_{ij}^{II}\frac{\Delta t}{4}} e^{\Psi_{ij}^I\frac{\Delta t}{2}} e^{\Psi_{ij}^{II}\frac{\Delta t}{4}}$,

$$\begin{aligned} e^{\Psi_{ij}^I\frac{\Delta t}{2}} u_{ij} &= u_{ij} e^{\beta_{ij} \Delta t/2} + \alpha_{ij} (e^{\beta_{ij} \Delta t/2} - 1) / \beta_{ij}, \\ e^{\Psi_{ij}^{II}\frac{\Delta t}{4}} u_{ij} &= u_{ij} / (1 - \gamma_{ij} u_{ij} \Delta t / 4), \\ e^{\Psi_{ii}^{II}\frac{\Delta t}{4}} u_{ii} &= u_{ii} / (1 - \zeta_{ii} u_{ii}^2 \Delta t / 2)^{1/2}. \end{aligned} \quad (7)$$

In such a way, starting from an initial configuration $\Gamma(0)$, the numerical solutions $n_i(t)$ and $u_{ij}(t)$ can be obtained for any time $0 < t \leq T$ by consecutively applying the actions according to Eqs. (5)–(7). Of course, DP (5) is not exact, so that $\mathcal{O}(\Delta t^3)$ -uncertainties arise. However, they can be reduced to an arbitrary small level by decreasing the size Δt of the time step. This completes the ISMD/KSA/DP approach.

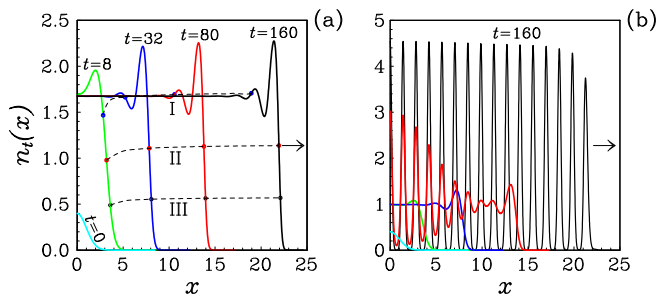


FIG. 1. Propagation of density distribution obtained by the ISMD [subset (a)] and MF [subset (b)] models with short-range dispersal.

Our ISMD/KSA/DP simulations were carried out in $d = 1$ at $L = 80$ and $h = 0.0125$ with $N = 6400$ and $\Delta t = 0.05$. Further increasing space and time resolution does not affect the solutions. The initial ($t = 0$) density distribution $n_0(x)$ was the Gaussian centered at $x = 0$ with $c_0 = 1$ and $\sigma_0 = 1$. Then $n_t(-x) = n_t(x)$, and, thus, $n_t(x)$ will be presented only for $x \geq 0$. Since we have up five parameters of the model, m , c_{\pm} , and σ_{\pm} , Eqs. (1) and (2) can describe various systems in different areas. We consider two characteristic examples.

The first is a system (of type 1) with short-range dispersal or long-range competition ($\sigma_+ \ll \sigma_-$) and small mortality ($m \ll c_+$). This was modeled by the square kernels with $\sigma_+ = 0.1$ and $\sigma_- = 1$ at $c_{\pm} = 1$ and $m = 0.01$. The second example (type 2) is opposite to the first one in the sense that it involves short-range competition or long-range dispersal ($\sigma_- \ll \sigma_+$) by choosing the Gaussian kernels with $\sigma_- = 0.1$ and $\sigma_+ = 1$ at the same $c_{\pm} = 1$ and $m = 0.01$.

The ISMD/KSA/DP results for density distribution $n_t(x)$ are shown in Figs. 1a and 2a for types 1 and 2, respectively, at five values of t . The MF data (type 1) are presented in Fig. 1b. From Fig. 1 we see that the MF approximation incorrectly predicts a periodic structure with deep amplitude modulation in a steady state at $t \gtrsim 160$. On the other hand, no such pattern arises within the accurate ISMD method. Here, with increasing t , the function $n_t(x)$ becomes flat in x near $x = 0$, while a strong oscillating-like inhomogeneity is maintained at the wavefront of the propagation. This striking difference can be explained by the fact that the MF approach completely neglects any spatial correlations by assuming $g_t(x, y) \equiv 1$. For type 2, the ISMD density profiles are more smooth (cf. Figs. 2a and 1a) and similar in shape with MF ones (not shown) but significantly larger than the latter in amplitude.

The total number of entities $N(t) = \int n_t(x) dx$ and their mean squared displacement $\langle x^2 \rangle(t) = \int x^2 n_t(x) dx / N(t)$ are plotted in Fig. 2b versus t . We see that the MF model appreciably underestimates values of $N(t)$ for both the types. The ISMD function $\langle x^2 \rangle$ of type 1 begins to depend linearly on t in a steady state after a relaxation time of $t \sim 32$. The linearity $\langle x^2 \rangle \sim t$ indicates about a diffusive-like behavior as in the limit $\sigma_+ \rightarrow 0$. However, in this limit the distribution functions will differ drastically from those of Figs. 1a and 2a. For type 2, we have $\langle x^2 \rangle \sim t^2$ in a steady state at $t \gtrsim 24$, meaning

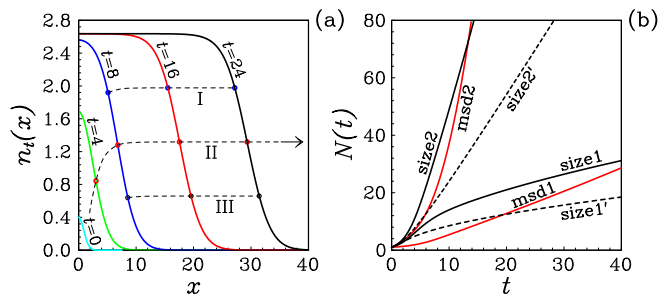


FIG. 2. (a) The same as for Fig. 1a but for short-range competition; (b) The ISMD (solid curves) and MF (dashed curves) population size $N(t)$ and mean squared displacement of entities for systems 1 and 2.

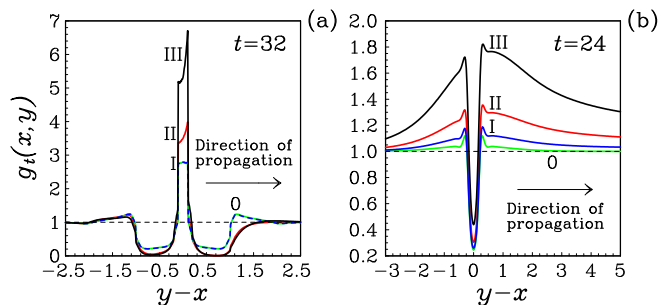


FIG. 3. The ISMD inhomogeneous pair correlation functions at $x = 0$ and in the the wavefront region ($x = x_{I,II,III}$) for short-range dispersal [subset (a)] and short-range competition [subset (b)].

that a regular regime takes place with $N \sim t$.

The inhomogeneous pair correlation functions $g_t(x, y) = u_t(x, y) / (n_t(x)n_t(y))$ are plotted in Fig. 3 at $t = 32$ (type 1) and $t = 24$ (type 2) as depending on $y - x$ for $x = 0$ and three wavefront points $x = x_{I,II,III}$. The latter were chosen such that $n_t(x_{I,II,III})$ decreases to the levels $3/4$, $1/2$, and $1/4$ with respect the maximum of n_t at given t (see circles connected by dashed curves in Figs. 1a and 2a). Fig. 3 demonstrates that $g_t(x, y)$ can significantly deviates from the MF value 1. Note that the initial condition $g_0(x, y) = 1$ with no pair correlations was utilized at $t = 0$. These correlations are quickly reproduced owing the interactions, so that already at $t \gtrsim 32$ or $t \gtrsim 24$ we obtain a steady-state behavior.

For type 1, we observe a strong clustering, $g_t(x, y) \gg 1$, of entities in the narrow regions $|y - x| \lesssim \sigma_+$ at the wavefront ($x = x_{I,II,III}$) of the density propagation, see Fig. 3a. With increasing distance $|y - x|$, the clustering suddenly transforms into a wide region of deep disaggregation, $g_t \approx 0$. In the homogeneous region ($x = 0$) these effects are not so pronounced. Note also that $g_t(0, -y) = g_t(0, y)$, whereas $g_t(x, y)$ is an asymmetric function in $y - x$ at $x \neq 0$. For type 2, the correlation function exhibits a narrow region of disaggregation at $|y - x| \sim 0$, where $g_t(x, y) \ll 1$ (look at Fig. 3b). Near $|y - x| \gtrsim \sigma_+/2$, the disaggregation changes to a moderate clustering ($g_t \sim 2$). At the wavefront ($x = x_{I,II,III}$), the spatial correlations are maintained up to long distances $|y - x| \sim 10 - 20$, where $g_t(x, y)$ decreases to its asymptotic

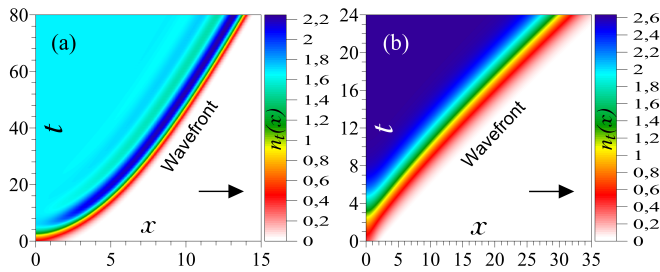


FIG. 4. The ISMD wavefront dynamics for short-range dispersal [subset (a)] and short-range competition [subset (b)].

value 1 very slowly with increasing $|y - x|$. This effect becomes stronger in the direction of propagation. On the other hand, no such long tails are detected in the homogeneous region $x = 0$, where $g_t(x, y) \rightarrow 1$ already at $|y - x| \gtrsim 3$, just as in Fig. 3a for type 1 at any x .

The wavefront dynamics is shown in detail in Fig. 4. We see that the structure of the wavefront regions is quite different for the two cases. As for the pair correlation functions, this difference is caused by the different forms of the interactions. Note that having $n_t(x)$, the spreading speed can be calculated as $v_t(x) = -(dn_t(x)/dt)/(\partial n_t(x)/\partial x)$.

Our investigations show that the previously known methods are unsuitable for solving the ISMD equations. The difficulty is that these methods are constructed on finite-difference schemes. Because of the numerical errors, unphysical negative solutions appear in these schemes for spatial regions, where the distribution functions are close to zero. The negative deviations are quickly accumulated step by step, and the computations fail. Instead, in the ISMD/KSA/DP approach the time evolution is performed by the analytical DP product of the exponential transformations which guaranty the positiveness. The latter is also inherent to the third-order KSA closure. Other known closures of lower orders, cannot, in general, ensure positive solutions and, thus, are not appropriate.

The DP technique developed here can be considered as the first extension of the powerful decomposition methodology [23, 24], widely used in molecular dynamics simulations of liquids, to the field of population dynamics. Its powerfulness is provided by the preservation of characteristics features inherent in exact solutions, such as reversibility and symplecticity of flow in phase space for liquids or positiveness of distributions for population systems. Other techniques, such as the Liouville formalism, concepts of hierarchies for kinetic equations, the KSA closure, all taken from non-equilibrium statistical physics of liquids, were also exploited in our work.

In summary, we have derived a novel ISMD/KSA/DP approach for computer simulations of spatially inhomogeneous population dynamics. It is based on the DP technique to solve numerically the kinetic equations for spatial moments of the distribution by splitting the time evolution operator into analytically solvable parts. As a result, the first ISMD modeling has been carried out for some population systems. This has enabled us to predict new effects which can take place in real

populations. They include the possible presence of asymmetric long tails in the inhomogeneous pair correlation functions, as well as the coexistence of strong clustering and deep disaggregation in the wavefront of spatial propagation.

The ISMD/KSA/DP approach can readily be adapted to more complex ISMD models [11, 12] by including neighbour-dependent birth, motility, and directionally biased movement. The KSA approximation can be improved by solving additionally the third kinetic equation from the hierarchy. The simulations can also be expanded to higher dimensions. All these questions will be the subject of our future researches.

-
- [1] J. D. Murray, *Mathematical Biology* (Springer-Verlag, New York, 1993).
 - [2] B. M. Bolker, In *Ecology, Genetics, and Evolution in Metapopulations*, edited by I. Hanski and O. Gaggiotti (Academic, New York, 2004).
 - [3] M. Iannelli and A. Pugliese, *An Introduction to Mathematical Population Dynamics* (Springer, New Delhi, 2014).
 - [4] B. Bolker and S. W. Pacala, *Theor. Popul. Biol.* **52**, 179 (1997).
 - [5] U. Dieckmann and R. Law, in *The Geometry of Ecological Interactions: Simplifying Spatial Complexity*, edited by U. Dieckmann, R. Law, and J. A. J. Metz (Cambridge University Press, Cambridge, 2000).
 - [6] D. J. Murrell, U. Dieckmann, and R. Law, *J. Theor. Biol.* **229**, 421 (2004).
 - [7] D. A. Birch and W. R. Young, *Theor. Popul. Biol.* **70**, 26 (2006).
 - [8] T. P. Adams, E. P. Holland, R. Law, M. J. Plank, and M. Raghieb, *Ecology* **94**, 2732 (2013).
 - [9] M. J. Simpson and R. E. Baker, *Bull. Math. Biol.* **77**, 581 (2015).
 - [10] M. J. Plank and R. Law, *Bull. Math. Biol.* **77**, 586 (2015).
 - [11] R. N. Binny, M. J. Plank, and A. James, *J. Royal Soc. Interface* **12** (2015), 10.1098/rsif.2015.0228
 - [12] R. N. Binny, P. Haridas, A. James, R. Law, M. J. Simpson, and M. J. Plank, *PeerJ* 4:e1689 (2016), 10.7717/peerj.1689.
 - [13] W. R. Young, A. J. Roberts, and G. Stuhne, *Nature* **412**, 328 (2001).
 - [14] R. Law, D. J. Murrell, and U. Dieckmann, *Ecology* **84**, 252 (2003).
 - [15] R. Law, J. Illian, D. F. R. P. Burslem, G. Gratzler, C. V. S. Gunatilleke, and I. A. U. N. Gunatilleke, *J. Ecol.* **97**, 616 (2009).
 - [16] D. J. G. Agnew, J. E. F. Green, T. M. Brown, M. J. Simpson, and B. J. Binder, *J. Theor. Biol.* **352**, 16 (2014).
 - [17] M. A. Fuentes, M. N. Kuperman, and V. M. Kenkre, *Phys. Rev. Lett.* **91**, 158104 (2003).
 - [18] D. Finkelshtein, Y. Kondratiev, Y. Kozitsky, and O. Kutoviy, *Eur. Phys. J. Special Topics* **216**, 107 (2013).
 - [19] D. Finkelshtein, Y. Kondratiev, and Y. Kozitsky, *Math. Models Meth. Appl. Sci.* **25**, 343 (2015).
 - [20] Y. E. Maruvka and N. M. Shnerb, *Phys. Rev. E* **73**, 011903 (2006).
 - [21] R. Law, J. Illian, D. F. R. P. Burslem, G. Gratzler, C. V. S. Gunatilleke, and I. A. U. N. Gunatilleke, *J. Ecol.* **97**, 616 (2009).
 - [22] A. Ben-Naim, *Journal of Advances in Chemistry* **1**, 27 (2013).
 - [23] I. P. Omelyan, I. M. Mryglod, and R. Folk, *Phys. Rev. Lett.* **86**, 898 (2001).
 - [24] I. Omelyan, I. Mryglod, and R. Folk, *Comput. Phys. Commun.* **151**, 272 (2003).